Journal of Molecular Catalysis A: Chemical 301 (2009) 61–66

Contents lists available at ScienceDirect

Journal of Molecular Catalysis A: Chemical

journal homepage: www.elsevier.com/locate/molcata

DFT-ONIOM study of Au/ZSM-5 catalyst: Active sites, thermodynamic and vibrational frequencies

Anibal Sierraalta[a,*], Paola Alejos[a], Elena Ehrmann[b], Leonardo J. Rodriguez[c], Yetziree Ferrer[c]

[a] Laboratorio de Química Computacional, Centro de Química, Instituto Venezolano de Investigaciones Científicas, Apartado 21827, Caracas 1020-A, Venezuela
[b] Departamento de Procesos y Sistemas, Universidad Simón Bolívar, Valle de Sartenejas, Baruta-Edo Miranda, Venezuela
[c] Laboratorio de Química Teórica y Computacional, Departamento de Química, Facultad Experimental de Ciencias, Apartado 526, Maracaibo, Venezuela

ARTICLE INFO

Article history:
Received 12 August 2008
Received in revised form 13 October 2008
Accepted 5 November 2008
Available online 14 November 2008

Keywords:
ONIOM
ZSM-5
CO
NO
Gold
Au
Zeolite
DFT
FTIR

ABSTRACT

Density functional and ONIOM calculations were carried out to investigate the possible active sites of Au(I) ion-exchanged ZSM-5 catalysts. Adsorption energies and vibrational frequencies of CO, NO, NO_2, SO_2, H_2O, NH_3, CH_3NH_2 and CH_3SH molecules were analyzed. For first time the existence of two active sites in Au/ZSM-5 is shown; one of them is responsible for the high and the other for the low CO and NO adsorption frequencies. The analysis of adsorption ΔG shows that Au(I) behaves like a soft acid; therefore, there will be a preferential adsorption of soft bases over hard bases. The interaction with NH_3 is thermodynamically very favored, mainly due to the hydrogen bond formation between the NH_3 hydrogen atoms and the oxygen atoms of the zeolitic framework.

1. Introduction

One of the main targets in environmental catalysis is the elimination of nitrogen oxides emissions, a dangerous mixture of NO and NO_2. These nitrogen oxides or NO_x are produced by mobile and stationary sources and are pollutants that severely damage air quality due to photochemical smog formation. A main goal is to find catalysts capable of facilitating the direct decomposition of NO_x to N_2 and O_2. These catalysts must be environmentally friendly and easy to handle. Among the many types of catalysts developed to eliminate the NO_x, $DeNO_x$ catalyst are the metal-exchanged zeolites. Many metal–zeolite combinations have been studied in the search for better catalysts, as for example Cu/ZMS-5 [1–3], Fe, Co and Pd over ZSM-5 [4–7], Ag over MOR, MFI or BEA [8,9], etc.

Gold has long been regarded as a poor catalyst, but recent results show that supported gold has good potential as heterogeneous catalyst. For instance, the discovery of unique activity of gold nanoparticles in CO oxidation at low temperature [10–12] has stimulated the research on gold catalysts. Sachtler et al., showed that Au/MFI catalyzes the decomposition of N_2O to N_2 even in the presence of O_2 [13]. Bond and Thompson [14] and Haruta [10] reported that highly dispersed gold catalyzes reactions such as CO oxidation and NO reduction. Ichikawa et al. [15] showed that the Au/ZSM-5 catalysts reduce the NO to N_2 in the presence of oxygen.

To explain the catalytic activity of Au over zeolites, different species with different oxidation states and structures have been proposed in the literature. Ichikawa et al. [16,17], used CO adsorption measured with FTIR, to study Au/NaY, Au/Na-MOR, and Au/Na-ZSM-5, and concluded that Au(I) is the dominant active site on which the reactions takes place. Sachtler et al. [13] used FTIR, XRD, and CO-TPR to analyze the Au/MFI system and concluded that gold is present mainly as both, Au(I) and Au(III). Despite experimental studies, many key questions remain unanswered: Where are the Au(I) ions located inside the zeolite framework? Which species are bound to Au(I) during the reaction, and how stable are these species? How easy is the interconversion of these species? How are the N–N and the O–O bonds formed? What particular steps in the reaction pathway affect catalytic activity and what steps hinder it? In the present work we analyze, from the quantum chemistry point of view, the physical–chemical properties and reactivity of Au(I) supported on ZSM-5 zeolite. The aim of the present work is to aid in the understanding of the nature of the Au/ZSM-5 active sites.

* Corresponding author.
E-mail address: asierral@ivic.ve (A. Sierraalta).

1381-1169/$ – see front matter © 2008 Elsevier B.V. All rights reserved.
doi:10.1016/j.molcata.2008.11.008

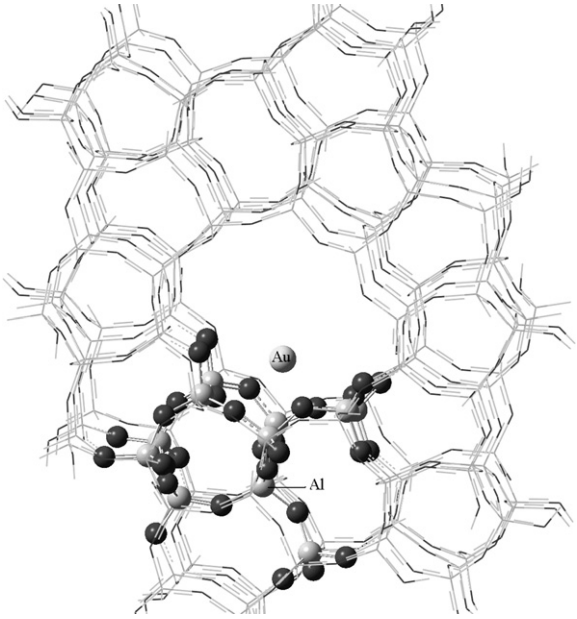

Fig. 1. Au-T8 site. High level: ball and stick. Low level: wireframe. Dark spheres: O atoms. Light grey spheres: Si atoms.

2. Computational details and models

All geometry optimizations, energy and frequency calculations were performed using Gaussian-03 program [18]. The lower energy structures were obtained using the two-layer ONIOM2 methodology. Universal force field approach (UFF) was employed for the low level calculations with no charge assigned to atoms while for the high level, the calculations were performed using the DFT approach (B3LYP) with the LANL2DZ basis set with its corresponding pseudopotentials for H, Si, Al, and O atoms belonging to the zeolite model ZSM–5. The relativistic Stevens effective core potential (CEP-121) with its corresponding basis set was employed for Au; and the full-electron 6-31+G* basis set for, NO, NO_2, SO_2, H_2O, NH_3, CH_3NH_2 and CH_3SH molecules. For the CO molecule, the full-electron 6-31+G with $\alpha_d(C) = 0.335884$ and $\alpha_d(O) = 0.535903$ basis set was used. This basis set reproduces the experimental metallic carbonyls frequencies with a standard deviation of $\pm 6\,cm^{-1}$ [19].

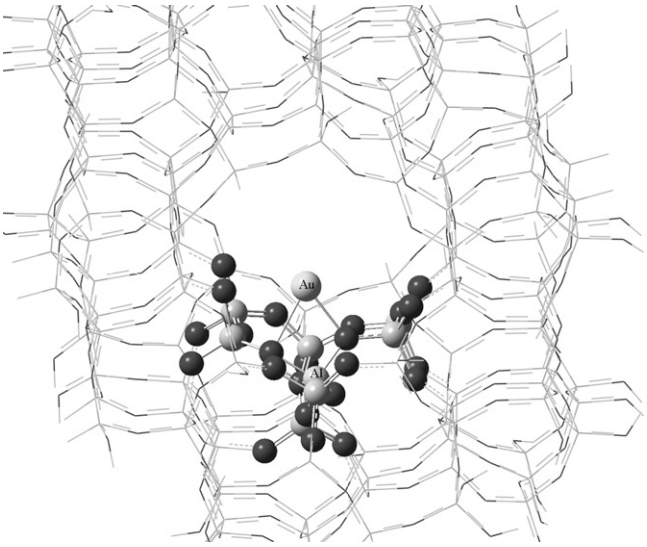

Fig. 3. Au-T7 site. High level: ball and stick. Low level: wireframe. Dark spheres: O atoms. Light grey spheres: Si atoms.

Thermodynamic property calculations; that is, ΔG and ΔH value calculations, were performed at 298.15 K using only the high level model.

Inside the ZSM-5 unit cell there are twelve Si types or T sites. A model for each T sites was generated substituting the Si by one Al atom. Due to the heterogeneity of the T sites, the 12 models corresponding to the 12 T sites contain different number of tetrahedrons in the high level model. Thus, there are 11 tetrahedrons for the T3, T4, T8 and T11 site models, 9 tetrahedrons for the T2, T6, T9 and T10 site models, and 8 tetrahedrons for the T1, T5, T7, and T12 site models. To model the Au/ZMS5 catalyst's active sites, one Au atom was placed on each T site. This generates a total of 12 Au–Tn structures to be studied. Figs. 1–4 show some of the models used in this work. A cluster model with a total number of 593 atoms was used to model the ZSM-5 zeolite. The cluster edges were terminated with H atoms to satisfy the edge atom valences. Similarly, for the high-level calculations, H atoms were used to satisfy the terminal atom valences.

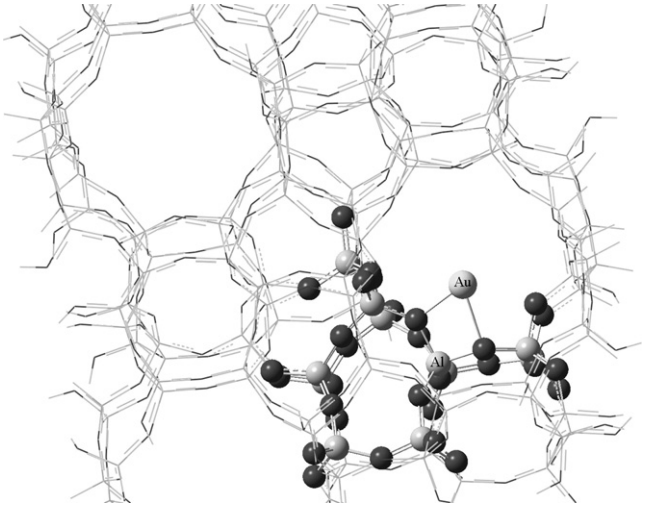

Fig. 2. Au-T11 site. High level: ball and stick. Low level: wireframe. Dark spheres: O atoms. Light grey spheres: Si atoms.

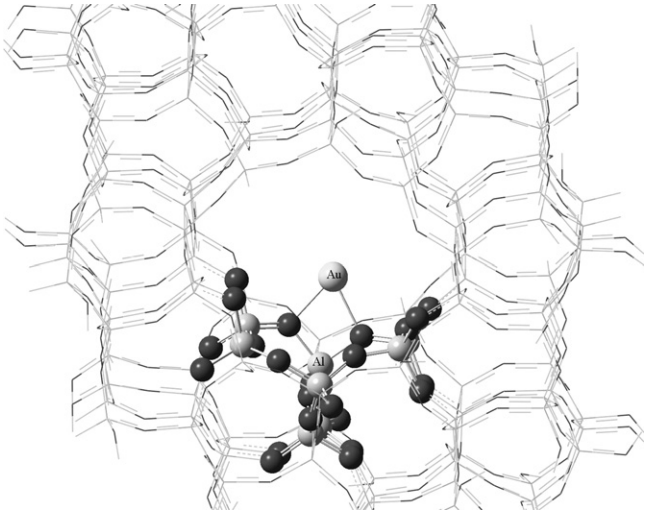

Fig. 4. Au-T12 site. High level: ball and stick. Low level: wireframe. Dark spheres: O atoms. Light grey spheres: Si atoms.

3. Results and discussions

3.1. Interaction with CO

When modeling the catalyst's possible active sites, it is necessary to compare calculated values with the experimental results to validate the model. Among available experimental data, the C–O stretching frequency has long been used as a monitor of structure and bonding in transition metal carbonyl complexes, as well as to determine and characterize the active sites of the catalysts. The CO stretching frequency is sensitive to the molecular environment of the bound CO because the extent of backbonding or π-backdonation is significantly altered by the surroundings. Therefore, to choose reasonable active site models for the highly dispersed Au/ZSM-5 catalyst, Quantum Chemistry calculations for CO adsorbed on Au in the different T sites were performed.

According to the reported experimental results, after exposing Au/ZSM-5 to CO at room temperature two intense FTIR bands appear; one reported at 2190 [13] and 2192 [16] cm^{-1}, and the other one reported at 2176 [13] and 2170 cm^{-1} [17]. Additionally, a weak shoulder at 2160 cm^{-1} has been reported [17] and attributed to the CO chemisorption on the Au(I) generated on the external surface of ZSM-5. Table 1 presents the calculated vibrational frequencies for carbonyl adsorbed on Au, on the twelve T sites of Au/ZSM-5. To test if the size of the high level region has important effects on the vibrational frequencies reported in Table 1, calculations with an increased high level region that includes a complete ring structure (see Figs. 5 and 6), were performed on the Au-T11 and the Au-T2 models. The results show that the difference between the new CO vibrational frequencies obtained with the larger models, ν_{CO}(COAu-T11-large) = 2164 cm^{-1} and ν_{CO}(COAu-T2-large) = 2166 cm^{-1}, and those reported on Table 1 are within the range of the calculation error (±6 cm^{-1}) Consequently, this suggests that the models with medium size high-level regions are adequate for the studies reported on this work.

The results reported on Table 1 show that only COAu-T8 is able to reproduce the vibrational frequency of 2192 cm^{-1}; hence, Au-T8 is a good candidate to represent one of the possible Au/ZSM-5's active sites. COAu-T11 and COAu-T12 reproduce the experimental value of 2170 cm^{-1} whereas COAu-T4, COAu-T5, COAu-T6 and COAu-T7 sites can be associated with the shoulder at 2160 cm^{-1}.

Table 1 shows that, in general, for all COAu–Tn sites, [AuCO] has a net charge of about +1. This is reasonable since the gold atom substitutes the H^+ proton that corresponds to the Brønsted acid site. The calculated ν_{CO} value for the free $AuCO^+$ species, 2237 cm^{-1}, is very different from those reported in Table 1 however; it is in good agreement with the experimental value of 2236.8 cm^{-1} obtained with Laser ablation techniques [20]. Consequently, this suggests that there is an important effect of the zeolite structure on the ν_{CO} of the $[AuCO]^+$ moiety.

Table 1
CO vibrational frequencies ν_{CO}, angles Au–C–O, net charges on CO (Q_{CO}) and AuCO moiety ($Q_{[AuCO]}$), and Au^+ binding energy (BE).

Site	ν_{CO}, cm^{-1}	Au–C–O, °	Q_{CO}, a.u.	$Q_{[AuCO]}$, a.u.	BE, kcal/mol
COAu-T8	2194	175.1	+0.142	+0.842	−154.1
COAu-T11	2170	176.6	+0.108	+0.822	−161.8
COAu-T2	2169	162.5	+0.066	+0.814	−189.5
COAu-T5	2164	178.6	+0.099	+0.807	−176.0
COAu-T6	2163	160.8	+0.057	+0.818	−186.9
COAu-T7	2162	176.6	+0.092	+0.812	−177.0
COAu-T4	2157	177.8	+0.081	+0.800	−155.2
COAu-T1	2148	178.7	+0.068	+0.809	−179.0
COAu-T3	2148	179.8	+0.067	+0.802	−177.0
COAu-T12	2133	174.0	-0.006	+0.806	−180.7
COAu-T10	2123	179.1	-0.008	+0.794	−168.5
COAu-T9	2119	179.7	-0.010	+0.804	−182.2

Free ν_{CO} exp. = 2143 cm^{-1}; free ν_{CO} cal. = 2141 cm^{-1}.

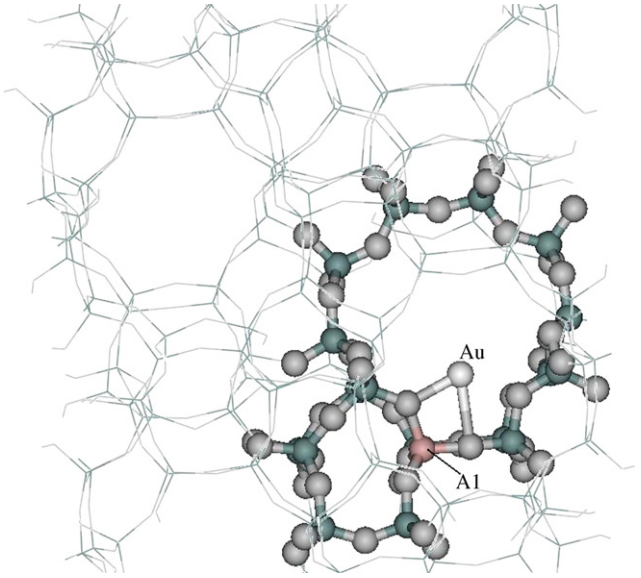

Fig. 5. Au-T11-large site. The high level region includes a complete ring structure. (see Fig. 2) High level: ball and stick. Low level: wireframe. Dark spheres: O atoms. Light grey spheres: Si atoms.

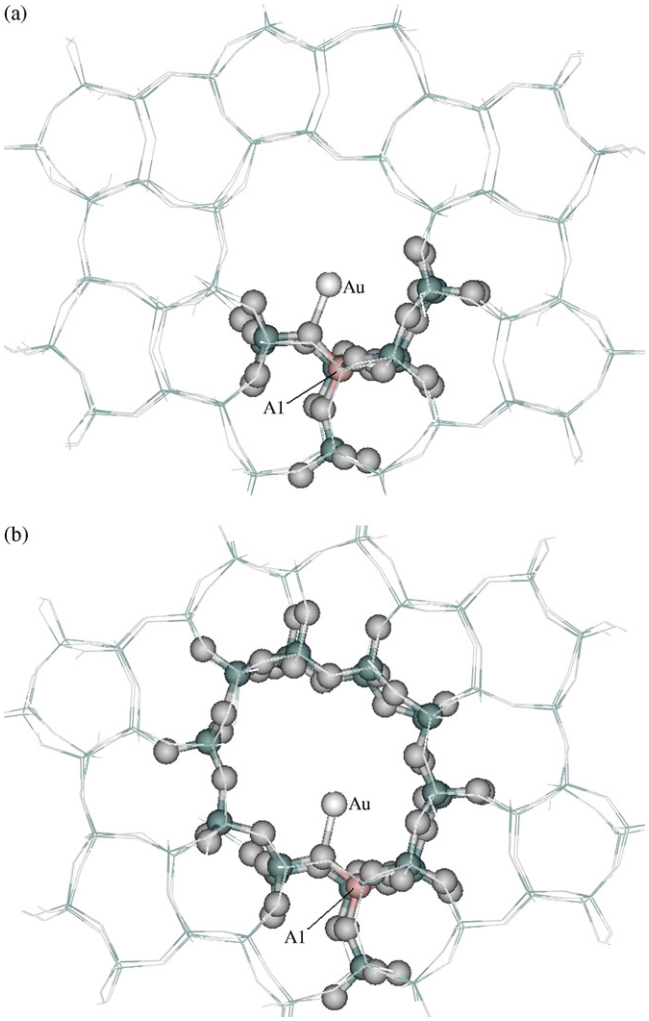

Fig. 6. High level: ball and stick. Low level: wireframe. Dark spheres: O atoms. Light grey spheres: Si atoms. (a) Au-T2 site and (b) Au-T2 site-large. The high level region includes a complete ring structure.

Table 2
ΔG and ΔH at 298.15 K for H_2O displacement by CO on different T sites.

Reaction site	ΔG, kcal/mol	ΔH, kcal/mol
$H_2OAu\text{-}T8 + CO \rightarrow COAu\text{-}T8 + H_2O$	−3.0	−1.9
$H_2OAu\text{-}T11 + CO \rightarrow COAu\text{-}T11 + H_2O$	−9.5	−7.3
$H_2OAu\text{-}T2 + CO \rightarrow COAu\text{-}T2 + H_2O$	−0.3	−5.4
$H_2OAu\text{-}T7 + CO \rightarrow COAu\text{-}T7 + H_2O$	−2.1	−2.6
$H_2OAu\text{-}T12 + CO \rightarrow COAu\text{-}T12 + H_2O$	−19.0	−18.0

It is well known that CO donates electrons to the metal via σ bond. This fills an Au d-orbital and increases the electron density at Au. To relieve the added electron density, the filled Au d-orbital interacts with the empty π^* orbital on the carbonyl ligand. As the π-backdonation becomes stronger, a decrease in the carbonyl stretching frequency in the IR is observed. According to Table 1, the lowest ν_{CO} corresponds to the COAu-T9 model which suggests that the π-backdonation is stronger for this site and consequently, the negative net charge on CO is the highest for this model. As the π-backdonation diminishes the negative net charge on the CO decreases, and the ν_{CO} increases. Thus, according to Table 1, the COAu-T8 exhibits the lowest degree of π-backdonation.

The former results show that each T site can be considered as a ligand with a different ability to accept back-donation. At sites with low back-accepting capability, such as the T9, T10, T12 models, the CO must accept more dπ electrons from the Au atom and therefore the ν_{CO} will be low. At high back-accepting capability sites, only a small or negligible π-backdonation from the Au to the CO and a high σ donation from the CO to the Au will occur. Therefore, the ν_{CO} will be high for T8, T11, T5 site models. Q_{CO} values for the COAu-T2 and COAu-T6 are low; this obeys to the fact that the C-O-Au angle is far from 180°; consequently, no backdonation is possible.

According to the former discussion regarding ν_{CO} values, the best candidates to accurately represent the Au/ZSM active sites are the T8, T11, T2, T5, T6 and T7 sites. In this work we choose T8, T11, T2, T7 and T12 sites to mimic the Au/ZSM-5 catalyst active sites. Although the calculated frequency for the COAu-T12 model site (2133 cm^{-1}) is far from the experimental value, it was included for comparison with previous studies [21,22].

To test the sites stability, Au^+ binding energy (BE) calculations were performed. The Au^+ binding energy is the energy necessary to separate the gold cation from its binding site. The analysis of the data reported in Table 1, indicate that the most stable sites i.e.; the sites with the highest BE are T2, T6, T9 and T2; while T4 and T8 are the least stables ones. No correlation was found between the BE and the ν_{CO} values. According to Sachtler et al. [13], CO slowly displaces water adsorbed on the Au/ZSM-5 catalyst at room temperature. To test if the T8, T11, T2 T7 and T12 model sites are able to reproduce this experimental fact, thermodynamic calculation for displacement reaction (1) were carry out. Results are presented in Table 2.

$$H_2OAu - Tn + CO \rightleftarrows COAu - Tn + H_2O \quad (1)$$

According to Table 2, the displacement of adsorbed H_2O by CO is thermodynamically favored ($\Delta G < 0$) on all sites. The correlation between the ΔG or ΔH values with the sites seems to be complex. For example, for the T2 site, $\Delta G = -0.3$ kcal/mol while for T12 it is −19.0 kcal/mol. To understand this behaviour, reaction (1) was divided into two steps: first, H_2O desorption, (reaction (2)) and next, CO adsorption (reaction (3)). The results are reported in Table 3.

$$H_2OAu - Tn \rightleftarrows AuTn + H_2O \quad (2)$$

$$Au - Tn + CO \rightleftarrows COAu - Tn \quad (3)$$

Table 3 shows that the H_2O adsorption energy, measured through ΔH, is greater for the T7 and T8 than for the T2, T11 and T12 sites. This could result from hydrogen bond formation. The molecular electronic density analysis shows that for H_2OAu-T8 and H_2OAu-T7, there are two hydrogen bonds between the water's H and the zeolite's oxygen, whereas for H_2OAu-T11, H_2OAu-T2 and H_2OAu-T12 there is only one. In consequence, the H_2O interaction energy is greater for H_2OAu-T8 and H_2OAu-T7 than for the other three sites.

Table 3
Adsorption ΔG and ΔH at 298.15 K for H_2O and CO en different T sites.

Reaction	ΔG, kcal/mol	ΔH, kcal/mol
$H_2OAu\text{-}T8 \rightarrow Au\text{-}T8 + H_2O$	32.2	42.2
$H_2OAu\text{-}T11 \rightarrow Au\text{-}T11 + H_2O$	13.7	26.4
$H_2OAu\text{-}T2 \rightarrow Au\text{-}T2 + H_2O$	17.1	27.5
$H_2OAu\text{-}T7 \rightarrow Au\text{-}T7 + H_2O$	32.5	42.4
$H_2OAu\text{-}T12 \rightarrow Au\text{-}T12 + H_2O$	18.4	29.7
$Au\text{-}T8 + CO \rightarrow COAu\text{-}T8$	−35.2	−44.1
$Au\text{-}T11 + CO \rightarrow COAu\text{-}T11$	−23.2	−33.7
$Au\text{-}T2 + CO \rightarrow COAu\text{-}T2$	−17.4	−32.9
$Au\text{-}T7 + CO \rightarrow COAu\text{-}T7$	−34.6	−45.0
$Au\text{-}T12 + CO \rightarrow COAu\text{-}T12$	−37.4	−47.7

On the other hand, the interaction of CO with Au(I) is stronger for T8, T7 and T12 than for T11 and T2, and in general, stronger than the corresponding interactions with H_2O (see Table 3) The balance between the CO adsorption and the H_2O desorption energies, including the hydrogen bond energies, produces the final values reported in Table 2 for ΔG and ΔH.

3.2. Interactions with soft and hard bases

It is well known that the Hard Soft Acid Base (HSAB) principle is an empirical principle that allows to predict the results of a given reaction and is very useful to understand and explain some experimental results, as well as to plan new chemical reactions. In order to classify the Au/ZSM-5 active sites as soft or hard acids, according to Pearson's rule or the HSAB, it is necessary to measure in some way the degree of the interaction between these active sites and soft and hard bases. Binding preference of the active site to hard bases indicates that Au/ZSM-5 behaves as a hard acid; whereas, binding preference to soft bases points towards a soft acid. Thus, adsorption ΔGs and ΔHs for CH_3SCH_3 (soft base) and CH_3OCH_3 (hard base) on Au/ZSM-5 were determined through Quantum Chemical calculations. Table 4 shows that, in general, the magnitude of the adsorption ΔH is larger and the reaction ΔG is more negative for CH_3SCH_3 than for CH_3OCH_3. Therefore, as long as ΔH and ΔG are relevant parameters to describe acid–base interactions, our results indicate that the Au/ZSM-5 active site behaves as a soft acid. Consequently, the Au/ZSM-5 will rather react with C_2H_4, R_2P, R_3As, R_2S, RNC, etc., than with R_2O, ROH, H_2O, etc. The experimental observation that CO displaces H_2O adsorbed on Au/ZSM-5 [13], can now be

Table 4
Adsorption ΔG and ΔH at 298.15 K for some hard and soft selected bases.

Reaction	ΔG, kcal/mol	ΔH, kcal/mol
$CH_3OCH_3 + Au\text{-}T8 \rightarrow (CH_3)_2OAu\text{-}T8$	−9.5	−21.0
$CH_3OCH_3 + Au\text{-}T11 \rightarrow (CH_3)_2OAu\text{-}T11$	−0.3	−13.6
$CH_3OCH_3 + Au\text{-}T2 \rightarrow (CH_3)_2OAu\text{-}T2$	0.6	−14.7
$CH_3OCH_3 + Au\text{-}T7 \rightarrow (CH_3)_2OAu\text{-}T7$	−4.4	−18.7
$CH_3OCH_3 + Au\text{-}T12 \rightarrow (CH_3)_2OAu\text{-}T12$	4.6	−13.4
$CH_3SCH_3 + Au\text{-}T8 \rightarrow (CH_3)_2SAu\text{-}T8$	−17.1	−31.2
$CH_3SCH_3 + Au\text{-}T11 \rightarrow (CH_3)_2SAu\text{-}T11$	−17.4	−29.9
$CH_3SCH_3 + Au\text{-}T2 \rightarrow (CH_3)_2SAu\text{-}T2$	−18.5	−32.8
$CH_3SCH_3 + Au\text{-}T7 \rightarrow (CH_3)_2SAu\text{-}T7$	−23.7	−34.0
$CH_3SCH_3 + Au\text{-}T12 \rightarrow (CH_3)_2SAu\text{-}T12$	−12.1	−27.2
$NH_3 + Au\text{-}T8 \rightarrow H_3NAu\text{-}T8$	−45.7	−54.5
$NH_3 + Au\text{-}T11 \rightarrow H_3NAu\text{-}T11$	−27.9	−38.1
$NH_3 + Au\text{-}T2 \rightarrow H_3NAu\text{-}T2$	−17.3	−26.9
$NH_3 + Au\text{-}T7 \rightarrow H_3NAu\text{-}T7$	−44.2	−53.0
$NH_3 + Au\text{-}T12 \rightarrow H_3NAu\text{-}T12$	−31.5	−45.6

Table 5
NO vibrational frequency (ν_{NO}) and adsorption ΔG and ΔH at 298.15 K on different T sites.

NO adsorption	[a] ν_{NO} (cm^{-1})	ΔG, kcal/mol	ΔH, kcal/mol
Au-T8 + NO → ONAu-T8	1873	−15.2	−23.0
Au-T11 + NO → ONAu-T11	1856	−1.8	−13.1
Au-T2 + NO → ONAu-T2	1824	−1.7	−14.9
Au-T7 + NO → ONAu-T7	1828	−13.8	−23.2
Au-T12 + NO → ONAu-T12	1780	−17.7	−27.5

[a] Calculated ν_{NO} were scaled by 0.9632. The standard uncertainty is 40 cm^{-1}.

easily explained. Water is a hard base while CO is a soft one; therefore, the active site, which is a soft acid, will preferentially bind to CO than to H_2O.

Table 4 shows the ΔG and ΔH values for the adsorption of the hard base NH_3. Noteworthy, unlike for the CH_3OCH_3 adsorption, NH_3 adsorption energies on Au/ZSM-5 sites are higher than the corresponding ones for the soft base CH_3SCH_3. The electronic density analysis showed that the NH_3 forms hydrogen bonds with the zeolite framework's oxygen atoms. Therefore, the total NH_3 adsorption energy, measured as adsorption ΔH, corresponds to the N–Au interaction plus the hydrogen bonds. This combination strongly stabilizes the NH_3 on the Au/ZSM-5, yielding high ΔH and ΔG values.

3.3. Interaction with NO, NO_2, and SO_2

Ichikawa et al. [17] showed that the Au(I)/ZSM-5 catalyst, when exposed to NO at 300 K in an IR cell, exhibits bands at 1820 and 1900 cm^{-1}. Table 5 shows the NO vibrational frequencies, ν_{NO}, for the selected T8, T11, T2, T7 and T12 sites. According to the results, ONAu-T2 and ONAu-T7 reproduce quite well the experimental ν_{NO} of 1820 cm^{-1}. The closest value to 1900 cm^{-1} was obtained for ONAu-T8, while ONAu-T11 presented an intermediate value between 1820 and 1900 cm^{-1}. These results, together with the adsorbed CO frequency results, Table 1, suggest that the Au/ZSM-5 catalyst possesses at least two different active sites. One of them, the Au-T8 site is responsible for the high ν_{CO} and ν_{NO} values. The other site, responsible for the low ν_{CO} and ν_{NO} values, can be represented by Au-T2, Au-T7 and Au-T11 models. The Au-T12 site does not reproduce the NO nor the CO frequencies.

Comparison between the results for the CO adsorption (Table 3) and for NO adsorption (Table 5) evidences the interaction with CO is thermodynamically more favored than the NO interaction. Therefore, CO can displace NO from the adsorption site.

Up to our knowledge, experimental studies of SO_2 and NO_2 adsorptions on Au/zeolites catalysts have not been reported in the literature until now. Some authors have reported a strong de-activation of the CO oxidation activity by SO_2 [23,24] and an extraordinary ability of Au/TiO_2 catalyst to adsorb and dissociate SO_2 [25] Regarding NO_2, Ichikawa et al. [15,17] proposed this molecule as an intermediate in the catalytic cycle of the NO reduction by Au/ZSM-5. Therefore, it is worthwhile to investigate the adsorption of SO_2 and NO_2 on Au/ZSM-5 catalysts.

Table 6 shows that, in general, the NO_2 adsorption is not thermodynamically favored, except for the Au-T7 and Au-T12 sites. This last site should not be considered since it does not reproduce the experimental ν_{CO} or the ν_{NO} values. For the Au-T7 site, $\Delta G < 0$ but for the Au-T2 site $\Delta G > 0$. This seems to indicate that not all possible sites responsible for the low CO and NO frequencies are actually good sites for NO_2 adsorption. Contrary to the NO_2 case, the SO_2 adsorption is thermodynamically favored at the Au-T8 site, which is responsible for the high ν_{CO} and ν_{NO}. The reason for this behavior seems to be related to the Au atom's oxidation degree and in the T site's capacity to withdraw or to donate charge from or to Au. In general, there is a charge transfer from the SO_2 to Au and from Au to NO_2. At the T8 site, the Au is more oxidized (Q_{Au} = +0.96e) than

Table 6
NO_2 and SO_2 adsorption ΔG and ΔH at 298.15 K on different T sites.

Reaction	ΔG, kcal/mol	ΔH, kcal/mol
NO_2 + Au-T8 → η^1-N O_2NAu-T8	−0.2	−13.2
NO_2 + Au-T11 → η^1-N O_2NAu-T11	2.0	−8.8
NO_2 + Au-T2 → η^1-N O_2NAu-T2	2.5	−9.6
NO_2 + Au-T7 → η^1-N O_2NAu-T7	−9.0	−19.8
NO_2 + Au-T12 → η^1-N O_2NAu-T12	−11.0	−21.9
NO_2 + Au-T8 → η^2-O NO_2Au-T8	6.1	−5.1
NO_2 + Au-T11 → η^2-O NO_2Au-T11	7.7	−6.5
NO_2 + Au-T2 → η^2-O NO_2Au-T2	9.2	−1.5
NO_2 + Au-T7 → η^2-O NO_2Au-T7	−8.8	−18.6
NO_2 + Au-T12 → η^2-O NO_2Au-T12	−9.2	−24.0
SO_2 + Au-T8 → η^1-S O_2SAu-T8	−6.2	−18.4
SO_2 + Au-T11 → η^1-S O_2SAu-T11	5.3	−7.6
SO_2 + Au-T2 → η^1-S O_2SAu-T2	4.6	−6.1
SO_2 + Au-T7 → η^1-S O_2SAu-T7	−7.4	−18.1
SO_2 + Au-T12 → η^1-S O_2SAu-T12	−7.5	−19.7
SO_2 + Au-T8 → η^2-O SO_2Au-T8	−14.2	−25.5
SO_2 + Au-T11 → η^2-O SO_2Au-T11	5.3	−6.2
SO_2 + Au-T2 → η^2-O SO_2Au-T2	7.1	−2.5
SO_2 + Au-T7 → η^2-O SO_2Au-T7	−2.3	−16.4
SO_2 + Au-T12 → η^2-O SO_2Au-T12	−7.5	−19.7

at the T7 site (Q_{Au} = +0.83e). Therefore, it is more difficult for the Au atom to transfer charge to NO_2 when at the T8 than at the T7 site. Consequently, the interaction is favored at the Au-T7 site over the Au-T8 site. On the other hand, the Au oxidation states at T2 and T7 are equal with (Q_{Au} = +0.83e) and without (Q_{Au} = +1.17e) the interaction with NO_2. However, there is a greater charge transfer from Au-T7 to NO_2 ($Q_{NO_2} = -0.45e$) than from Au-T2 ($Q_{NO_2} = -0.36e$) to NO_2. This reveals that the charge donation from the T Brønsted site to Au is greater at T7 than at T2. The electrons are less tight at T7 than at T2; therefore, T7 can donate more easily electrons to Au than T2. This charge supply from the T site stabilizes the oxidation state of the Au atom, allowing a greater net charge transfer to the NO_2 molecule and favoring the interaction. In consequence, the NO_2 adsorption ΔH magnitude is greater for Au-T7 than for Au-T2.

4. Conclusions

The most relevant features found in this work can be summarized as follows. (a) The CO and NO vibrational frequencies indicate that the Au/ZSM-5 catalyst has at least two different active sites. One of them is responsible for the high frequencies, ν_{CO} = 2192 cm^{-1} and ν_{NO} = 1900 cm^{-1} and can be represented by the Au-T8 site (ν_{CO} = 2194 cm^{-1} and ν_{NO} = 1873 cm^{-1}). The other one is responsible for the low frequencies, ν_{CO} = 2170 cm^{-1} and ν_{NO} = 1820 cm^{-1}. The theoretical results show that the responsible site for the low vibrational frequencies can be modeled by different sites such as: Au-T2 (ν_{CO} = 2169 cm^{-1} and ν_{NO} = 1824 cm^{-1}), Au-T7 (ν_{CO} = 2162 cm^{-1} and ν_{NO} = 1828 cm^{-1}), and Au-T11 (ν_{CO} = 2170 cm^{-1} and ν_{NO} = 1856 cm^{-1}). Therefore, it is not possible to know if the low CO and NO frequencies are consequence of a Au^+ localization on a single specific site such as for example T11, or the result of a distribution of the gold cations on two or three different sites, for example: T5 and T6 or T2, T7, and T11, that yield similar frequencies. More studies are needed to reach a conclusion. (b) The Au on ZSM-5 behaves likes a soft acid; therefore, soft bases such as CO, C_2H_4, R_2P, R_2S will bind to it preferentially over hard bases such as H_2O, R_2O, ROH. (c) The interaction with hard bases similar to NH_3 are thermodynamically very favored, mainly due, to the formation of hydrogen bonds between the NH_3 hydrogen atoms an the zeolitic framework oxygen atoms. (d) Each T sites has a different electron-donating capacity and back-accepting ability. This limits the amount of electrons that can

be transferred to the adsorbate and to the Au atoms. At soft sites, Au can transfer more electrons than at hard sites.

Acknowledgment

The authors acknowledge the financial support given by FONACIT G-2005000426 project.

References

[1] M. Shelef, Chem. Rev. 95 (1995) 209.
[2] H. Yahiro, M. Iwamoto, Appl. Catal. A 222 (2001) 163.
[3] S.A. Gomez, A. Campero, A. Martínez-Hernández, G.A. Fuentes, Appl. Catal. A 197 (2000) 157.
[4] M. Schidder, M.S. Kumar, K. Klementiev, M.M. Pohl, A. Brückner, W. Grünert, J. Catal. 231 (2005) 314.
[5] M. Devades, O. Kröcher, M. Elsener, A. Wokiaun, N. Söges, M. Pfeifer, Y. Demel, L. Mussmann, Appl. Catal. B Environ. 67 (2006) 187.
[6] C. Chupin, A.C. van Veen, M. Konduru, J. Despres, C. Mirodals, J. Catal. 241 (2006) 103.
[7] L.J. Lobree, A.W. Aylor, J.A. Reimer, A.T. Bell, J. Catal. 181 (1999) 189.
[8] J. Shibata, Y. Takada, A. Shichi, S. Satokawa, A. Satsuma, T. Hattori, Appl. Catal. B Environ. 54 (2004) 137.
[9] J. Shibata, K. Shimizu, Y. Takada, A. Shichi, H. Yoshida, S. Satokawa, A. Satsuma, T. Hattori, J. Catal. 227 (2004) 367.
[10] M. Haruta, Catal. Today 36 (1997) 153.
[11] J.C. Fierro-Gonzalez, J. Guzman, B.C. Gates, Topics Catal. 44 (2007) 103.
[12] A. Simakov, I. Tuzovskaya, A. Pestryakov, N. Bogdanchikova, V. Gurin, M. Avalos, M.H. Farıas, Appl. Catal. A: Gen. 331 (2007) 121.
[13] Z. Gao, Q. Sun, H. Chen, X. Wang, W.M.H. Sachtler, Catal. Lett. 72 (2001) 1.
[14] G.C. Bond, D.T. Thompson, Catal. Rev. 41 (1999) 319.
[15] T.M. Salama, R. Ohnishi, M. Ichikawa, Chem. Commun. 1 (1997) 105.
[16] M.M. Mohamed, T.M. Salama, M. Ichikawa, J. Colloid Interface Sci. 224 (2000) 366–371.
[17] S. Qiu, R. Ohnishi, M. Ichikawa, J. Phys. Chem. 98 (1994 2719).
[18] M.J. Frisch, G.W. Trucks, H.B. Schlegel, G.E. Scuseria, M.A. Robb, J.R. Cheeseman, J.A. Montgomery Jr., T. Vreven, K.N. Kudin, J.C. Burant, J.M. Millam, S.S. Iyengar, J. Tomasi, V. Barone, B. Mennucci, M. Cossi, G. Scalmani, N. Rega, G.A. Petersson, H. Nakatsuji, M. Hada, M. Ehara, K. Toyota, R. Fukuda, J. Hasegawa, M. Ishida, T. Nakajima, Y. Honda, O. Kitao, H. Nakai, M. Klene, X. Li, J.E. Knox, H.P. Hratchian, J.B. Cross, V. Bakken, C. Adamo, J. Jaramillo, R. Gomperts, R.E. Stratmann, O. Yazyev, A.J. Austin, R. Cammi, C. Pomelli, J.W. Ochterski, P.Y. Ayala, K. Morokuma, G.A. Voth, P. Salvador, J.J. Dannenberg, V.G. Zakrzewski, S. Dapprich, A.D. Daniels, M.C. Strain, O. Farkas, D.K. Malick, A.D. Rabuck, K. Raghavachari, J.B. Foresman, J.V. Ortiz, Q. Cui, A.G. Baboul, S. Clifford, J. Cioslowski, B.B. Stefanov, G. Liu, A. Liashenko, P. Piskorz, I. Komaromi, R.L. Martin, D.J. Fox, T. Keith, M.A. Al-Laham, C.Y. Peng, A. Nanayakkara, M. Challacombe, P.M.W. Gill, B. Johnson, W. Chen, M.W. Wong, C. González, J.A. Pople, Gaussian 03, Revision D. 02, Gaussian, Inc., Wallingford, CT, 2004.
[19] A. Sierraalta, G. Martorell, E. Ehrmann, R. Añez, Int. J. Quantum Chem. 108 (2008 1036).
[20] B. Liang, L. Andrews, J. Phys. Chem. A 104 (2000) 9156.
[21] A. Sierraalta, R. Hernández-Andara, E. Ehrmann, J. Phys. Chem. B 110 (2006) 17912.
[22] A. Sierraalta, R. Añez, M. Rosa-Brussin, J. Phys. Chem. A 106 (2002) 6851.
[23] K. Ruth, M. Hayes, R. Burch, S. Tsubota, M. Haruta, Appl. Catal. B: Environ. 24 (2000) L133.
[24] M.R. Kim, S.I. Woo, Appl. Catal. A: Gen. 299 (2006) 52.
[25] J.A. Rodriguez, G. Liu, T. Jirsak, J. Hrbek, Z. Chang, J. Dvorak, A. Maiti, J. Am. Chem. Soc. 124 (2002) 5242.